applied sciences

MDPI

Article

Effect to the Surface Composition in Ultrasonic Vibration-Assisted Grinding of BK7 Optical Glass

Pei Yi Zhao [1,*], Ming Zhou [2], Xian Li Liu [1] and Bin Jiang [1]

1 School of Mechanical and Power Engineering, Harbin University of Science and Technology, Harbin 150080, China; liuxianli@hrbust.edu.cn (X.L.L.); jiangbin@hrbust.edu.cn (B.J.)
2 School of Mechatronics Engineering, Harbin Institute of Technology, Harbin 150006, China; zhouming@hit.edu.cn
* Correspondence: zhao.py.630@gmail.com

Received: 10 December 2019; Accepted: 7 January 2020; Published: 10 January 2020

Featured Application: Authors are encouraged to provide a scientific support for controlling of machined surface composition in ultrasonic vibration assisted grinding of optical glass materials.

Abstract: Because of the changes in cutting conditions and ultrasonic vibration status, the proportion of multiple material removal modes are of uncertainty and complexity in ultrasonic vibration-assisted grinding of optical glass. Knowledge of the effect of machined surface composition is the basis for better understanding the influence mechanisms of surface roughness, and also is the key to control the surface composition and surface quality. In the present work, 32 sets of experiments of ultrasonic vibration-assisted grinding of BK7 optical glass were carried out, the machined surface morphologies were observed, and the influence law of machining parameters on the proportion of different material removal was investigated. Based on the above research, the effect of surface composition was briefly summarized. The results indicated that the increasing of spindle rotation speed, the decreasing of feed rate and grinding depth can improve the proportion of ductile removal. The introduction of ultrasonic vibration can highly restrain the powdering removal, and increase the proportion of ductile removal. Grinding depth has a dominant positive effect on the surface roughness, whereas the spindle rotation speed and ultrasonic amplitude both have negative effect, which was caused by the reduction of brittle fracture removal.

Keywords: surface composition; optical glass; ultrasonic vibration; grinding; influence law

1. Introduction

Optical glass is a typical hard and brittle material. Because of its unique excellent properties, it has a wide range of applications in the fields of optics, inertial confinement nuclear fusion, aerospace, and defense [1,2]. One of the most prominent features of optical glass materials is high brittleness and low fracture toughness. The critical cutting depth of the material is extremely small. When the instantaneous cutting depth of the abrasive grains did not reach the critical cutting depth, the material is removed by plastic deformation [3]. When the instantaneous cutting depth of the abrasive grains reached beyond the critical cutting depth, micro cracks are generated inside the material, as the micro cracks propagates onto the machined surfaces, the material was removed by brittle fracture [4] and powdering [5,6].

Ultrasonic vibration-assisted grinding has been used for precision machining of brittle materials because of the fact that the average cutting force and cracks propagation can be significantly reduced [7–9]. The effect of the process parameters on the process performances has been investigated experimentally [10–12]. After introducing ultrasonic vibration into the machining process, impact effect was induced while the tool cutting into the optical glass material [13]. The effect of process parameters on surface quality, such as surface roughness and machined surface composition may be different than that of conventional cutting [14]. To the best of our knowledge, there are few reports on the machined surface composition and materials removal modes.

In the past few years, domestic and foreign researchers have carried out a series of research on the removal of optical glass materials. Zhao conducted a scratching test by varying the cutting depth, based on this, he divided the material removal process into three parts: pure plastic flow, plastic and fracture mixture, and brittle fracture. Clear cutting chips and material deformation characteristics were found in his experiments. In addition, he also explained the cracks propagation directions, it was claimed that the initial radial cracks tend to propagate along twinning planes while the lateral cracks propagate along the basal plane [15]. Cao investigated the material removal and deformation characteristics by observing the scratched surface morphologies, he pointed that the scratch groove depth is deeper in ultrasonic vibration-assisted scratching [16]. Zhang researched the relationship between stress characteristics and cracks propagation directions based on a varied cutting-depth nanoscratching test [17], he also discussed the transition of material removal mode based on the observation of scratched grooves. In another research of Zhang, the differences of material removal in conventional grinding and ultrasonic vibration assisted grinding (UVAG) were investigated by observing machined surface morphologies by using atomic force microscope (AFM) and scanning electron microscope (SEM) [18]. He also compared the scratched grooves width and cracks propagation of varied scratching depth by conducting actual experiments and simulating scratching process [19]. Li focused on the influence of elastic recovery on scratched grooves morphologies. He pointed that elastic recovery may be a significant factor that affects machined surface quality in the actual grinding process [20]. However, many of the present researches related to material removal are based on the observation and analysis after scratching and indentation tests, which means the factors such as the coupling effects of cracks in actual grinding process, and the variation of grinding parameters, could not be easily taken into consideration.

In the ultrasonic vibration grinding process of optical glass, because of the huge number of abrasive grains on the surface of the grinding wheel, and the randomness of the size and shape, the protruding height of each abrasive grain is different, resulting in different instantaneous cutting depths during processing. Therefore, there are often plastic removal methods, brittle removal methods, and powder removal methods in the process. Moreover, under the combination of different processing parameters, the proportion of the above three material removal methods on the machined surface will also change, this change would be certainly depended on process parameters and grinding wheel parameters. The mapping relationship between them needs to be studied. Wang developed a critical function for crack propagation based on single grit scratching test, by using this function, he further presented a model for predicting the change of material removal mode. In his model, original crack density, strain rate, and grinding coolant are considered, the results showed that the crack damage depth would reach a maximum value while the material removal mode is semi-brittle [21]. Dai investigated the influence law of spindle rotation speed on grinding force and specific grinding energy, he also claimed that the cracks and brittle-fractured pits sizes would become enormous because of the transition of material removal mechanism (ductile regime to completely brittle regime) [22]. Gu has taken consideration of coupling effects of multiple abrasive grains on cracks propagation to simulate actual grinding process. He pointed that the micro cracks sizes would be significantly affected by the separation distance of two abrasive grains [23]. However, there are few reports on the mapping relationship between process parameters and material removal methods in the process of ultrasonic vibration grinding of optical glass.

When the material is removed in different ways, it will produce different processed surface topography, which will also produce different degrees of subsurface damage. Therefore, the proportion of these removal methods on the machined surface determines the final machined surface quality and subsurface damage. Although studies at home and abroad have been able to control the surface roughness [24–26], processing efficiency [27,28], force and energies [29,30] or damages [31] by adjusting the process parameters, for the precision machining of brittle materials that pay attention to the surface quality and subsurface damage at the same time, the intrinsic relationship between the proportion of the material removal modes and the process parameters and the parameters of the grinding wheel is still not clear. The effective control of the material removal modes proportion is the basis and key to exploring the technical measures to jointly improve the processing surface and subsurface quality.

In this paper, to comprehensively investigate the effect of grinding parameters and ultrasonic parameters to surface composition, 32 sets of experiments of ultrasonic vibration grinding of optical glass are carried out first. Second, based on the measurement results, the effect of grinding parameters and ultrasonic parameters on surface roughness was investigated, the changes of machined surface morphologies and the proportion of three material removal modes in different grinding parameters are analyzed. At last, the effect of processing parameters on surface composition in ultrasonic vibration-assisted grinding of optical glass is briefly summarized.

2. Experimental Setup

In order to investigate the effect of grinding and ultrasonic vibration parameters on surface composition and surface roughness, ultrasonic vibration-assisted grinding experiments of BK7 optical glass materials were carried out on a 5-axis precision ultrasonic machine center (DMG Ultrasonic 70-5 linear). The Schott ultrasonic hollow nickel electroforming diamond grinding wheel was used, whose diameter was 4 mm, average grain diameter was 64 um, and the diamond concentration was 100%. Automatic laser measuring device was used to measure the length and radius of the tool. The grinding tool oscillates along the axial direction of the spindle. The ultrasonic frequency of the cutting tool was detected by the machine tool measurement device and its value was 30,047 Hz. The BK7 optical glass material workpieces were in the form of cuboid with 50 mm in length, 50 mm in width, and 6 mm in height. In order to preclude the influence of coolant on machining process, grinding coolant was not used in these experiments. The glass workpiece was fixed to a steel plate using strong adhesive. After sticking, the object was allowed to stand for 24 h at room temperature. Experimental setup and scheme of the process kinematics is shown in Figure 1.

To extensively investigate the influencing law of machining parameters on surface composition and surface roughness, a single factor design was employed in the experiments. The spindle rotation speed, grinding depth, feed rate, and ultrasonic vibration amplitude were defined as the experimental parameters. Since the resonance frequency is the best vibration frequency of the cutting tool during the process of ultrasonic vibration machining, the ultrasonic frequency was not considered as the parameter during the experiments [32,33]. The concrete experimental parameters are given in Table 1. A total of 32 groups of experiments were carried out on BK7 optical glass based on this experimental design.

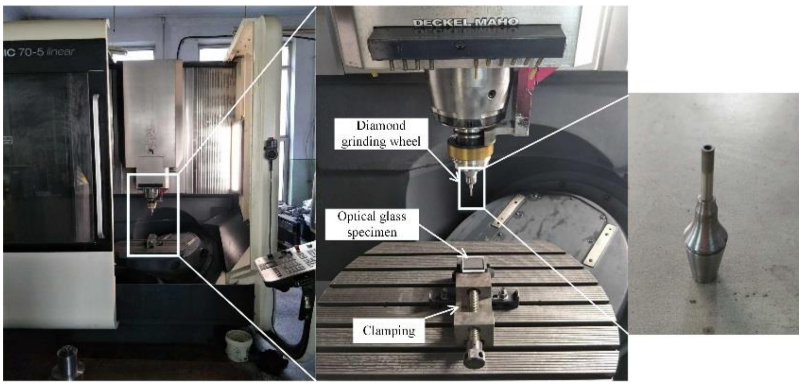

(**a**) Experimental setup

Figure 1. *Cont.*

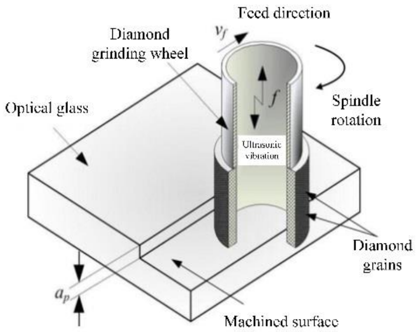

(**b**) Scheme of the process kinematics

Figure 1. Experimental setup and scheme of the process kinematics.

Table 1. Machining parameters in ultrasonic vibration assisted grinding experiments of BK7 optical glass.

Serial No.	Spindle Rotation Speed n/(rpm)	Feed Rate V_f/(mm/min)	Grinding Depth a_p/(μm)	Ultrasonic Amplitude A/(μm)
1	1000	110	60	7
2	3000	110	60	7
3	5000	110	60	7
4	7000	110	60	7
5	9000	110	60	7
6	11,000	110	60	7
7	13,000	110	60	7
8	15,000	110	60	7
9	11,000	10	60	7
10	11,000	30	60	7
11	11,000	50	60	7
12	11,000	70	60	7
13	11,000	90	60	7
14	11,000	110	60	7
15	11,000	130	60	7
16	11,000	150	60	7
17	11,000	110	10	7
18	11,000	110	20	7
19	11,000	110	30	7
20	11,000	110	40	7
21	11,000	110	50	7
22	11,000	110	60	7
23	11,000	110	70	7
24	11,000	110	80	7
25	11,000	110	60	0
26	11,000	110	60	1
27	11,000	110	60	2
28	11,000	110	60	3
29	11,000	110	60	4
30	11,000	110	60	5
31	11,000	110	60	6
32	11,000	110	60	7

After the experiments, the surface morphologies of the machined surfaces were observed by SEM, and the surface roughness of the machined surfaces were measured by AFM manufactured by Nanosurf Nanite, Switzerland, whose average error in the X/Y direction is less than 0.6%, the number of sampling lines set in the X/Y directions are both 256, the number of sampling points of each line is 256. In order to eliminate the random error, three sampling areas are taken randomly on the machined surface, and the average value is taken as the final result of surface roughness. The surface arithmetic mean deviation (*Sa*) is selected as an index for evaluating the quality of the machined surface, and the specific algorithm is shown in Equation (1).

$$Sa = \frac{1}{MN}\sum_{j=1}^{N}\sum_{i=1}^{M}|\eta ji| \quad (1)$$

where

η_{ij}—the protrusion height at the measuring point of the *i*th row and the *j*th column;
M—total number of rows in the measurement area;
N—total number of columns in the measurement area.

3. Results and Discussions

3.1. Analysis of the Effects in Surface Morphologies and Surface Roughness

3.1.1. Effect of Grinding Parameters on Surface Morphologies and Surface Roughness

To observe the details of morphologies on machined surfaces, 100 times zoomed images of the morphologies at spindle rotation speed of 1000 rpm and 15,000 rpm are shown in Figure 2a,b, respectively. Lots of brittle-fractured pits in large sizes was obviously observed on the machined surface at the spindle rotation speed of 1000 rpm. It can be seen that the density of brittle-fractured pits on the surface produced at a spindle rotation speed of 15,000 rpm is much higher than that generated at a spindle rotation speed of 1000 rpm. The amount of brittle-fractured pits in large sizes produced at n = 15,000 rpm is also found to be much less than that produced when n = 1000 rpm. According to Equation (1), the fluctuation of protrusion heights of brittle-fractured pits is much bigger than that of other areas on the machined surface, and, the existing of these areas could be the possible reason that surface roughness always is in big value when the spindle rotation speed is small.

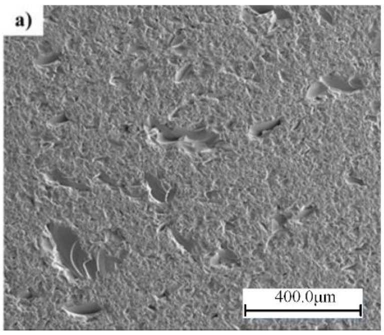

(**a**) 100 times zoomed image at n = 1000 rpm

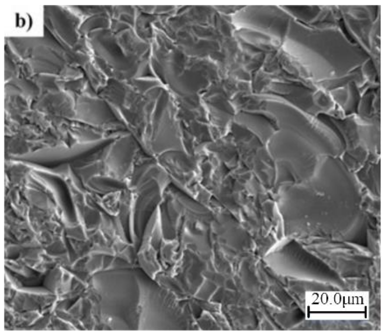

(**b**) 1000 times zoomed image at n = 1000 rpm

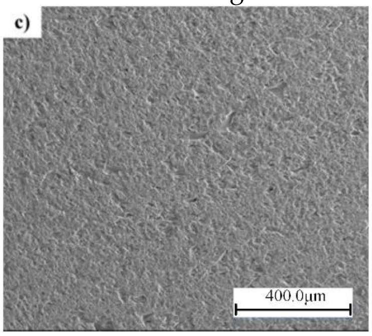

(**c**) 100 times zoomed image at n = 15,000 rpm

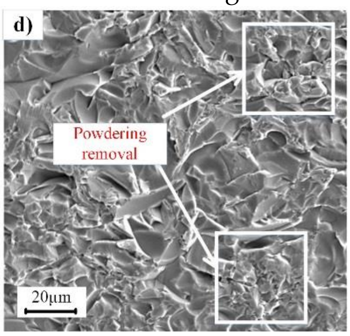

(**d**) 1000 times zoomed image at n = 15,000 rpm

Figure 2. Machined surface morphologies of optical glass at different spindle rotation speed.

After the obvious increasing of spindle rotation speed, the sizes of brittle-fractured areas overall decrease, and the machined surface becomes smooth. Meanwhile, the brittle-fractured pits in large sizes nearly disappear. In order to further observe the influence of spindle rotation speed on the proportion of different material removal modes, especially on the changing of powdering removal, another two images of same surface areas zoomed by 1000 times are shown in Figure 2b,d. From Figure 2b, slight powdering removal is found on the machined surface, and mainly consisted of fracture lumps in micron level and scraps in sub-micron level. These defects all covered on the machined surface but did not propagate onto the surface. After the spindle rotation speed changing to 15,000 rpm, the scraps in sub-micron level nearly disappear and the amounts of fracture lumps also decrease to a certain level, but they can still be found on the machined surface. Hence, a conclusion can be drawn, obvious change in spindle rotation speed can strongly influences not only the surface roughness, but also the proportion of powdering removal in sub-micron level, but cannot make the fracture lumps in micron level change obviously.

The influence law of feed rate on surface roughness is shown in Figure 3. It can be seen that the surface roughness has a rise as the feed rate increases. A possible reason for this change is that the increase of feed rate leads to the decrease of critical cutting depth of BK7 optical glass material [34]. Another reason is that the number of grinding times of a single abrasive grain during unit time decreases, to maintain the material removal rate in a certain level, the glass material will be removed in bigger volumes. While there is no change on other conditions, the above two reasons both will lead to the increase of grinding force and the proportion of brittle removal, surface roughness thus becomes bigger.

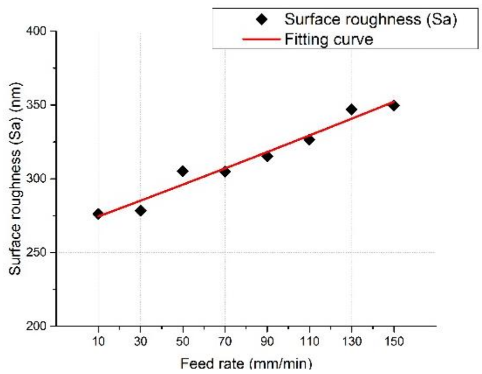

Figure 3. Influence of feed rate on surface roughness.

It also can be seen from Figure 3, while the feed rate changing from 10 mm/min to 150 mm/min, the surface roughness only increased by around 75 nm. This means, although surface roughness is widely used to assess machined surface quality, for optical glass material, the surface roughness may not be such sensitive to cutting parameters than that in machining of other materials. On the contrary, the proportion of material removal modes may be more efficient to justify the surface quality. Thus, the effect of feed rate on the proportion of material removal modes should also be investigated.

For a deeper observation, 300 times zoomed images were selected to investigate the machined surfaces morphologies of optical glass material, as shown in Figure 4. It can be seen that the material removal sizes on machined surfaces tend to be well-distributed at the feed rate of 10 mm/min, and no obvious removal areas in large sizes are found. But after the feed rate changing to 110 mm/min, several brittle-fractured pits are found on the machined surface and their sizes are obviously larger than that of other features. It is believed that the brittle-fractured pits mentioned above mainly consist of incompletely developed willow leaf shaped pits and incompletely developed double sector shaped pits.

Notably, through the observation on 1000 times zoomed images of the machined surface, it can be seen that the powdering material removal can be easily found on the machined surface at the feed rate of 10 mm/min. Quite a few fracture lumps in micron level and scraps in sub-micron level produced by powdering material removal covered on the machined surface, and their proportion seems quite large. However, after the feed rate changing to 110 mm/min, powdering material removal is found to be much less, instead, brittle-fractured pits were induced onto the machined surface. Thus, the change of feed rate has a significant influence on the material removal modes, also has a great effect on the proportion of each removal mode.

According to the measured results of surface roughness, the surface roughness (*Sa*) of machined surface showed in Figures 2c and 4a are 276.15 nm and 300.20 nm, respectively. Although there only exists a difference of 24.15 nm, their surface morphologies and material removal mechanism are much different. It can be seen from Figure 4c that the machined surface consists of small ductile and brittle removal pits. But no obvious powdering removal is found. Since only spindle rotation speed and feed rate changed in Figures 2c and 4a, respectively, the change of surface morphologies and material removal mechanism thus might be related to the trajectories of abrasive grains, which can also prove that the changes of spindle rotation speed and feed rate would have a significant influence not only on the morphologies and sizes but also on material removal modes. Thus, a conclusion can be drawn, at the combination of high spindle rotation speed and high feed rate, optical glass material is removed mainly by incompletely developed willow leaf shaped pits, incompletely developed double sector shaped pits and their combination in large sizes, supplemented by lumps in micron level. At the combination of high spindle rotation speed and low feed rate, optical glass material is removed mainly by lumps at the micron level, supplemented by completely and incompletely developed willow leaf shaped pits in small sizes.

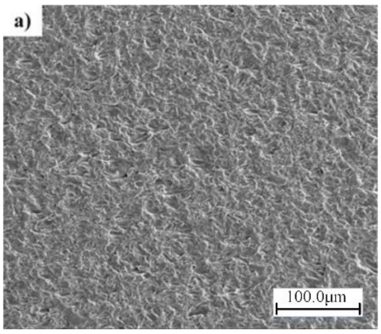

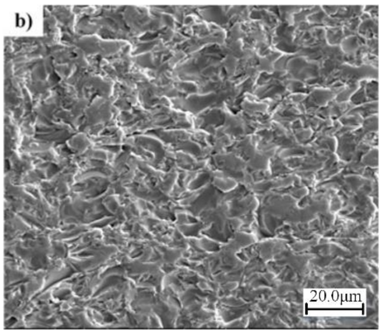

(**a**) 300 times zoomed image at V_f = 10 mm/min (**b**) 1000 times zoomed image at V_f = 10 mm/min

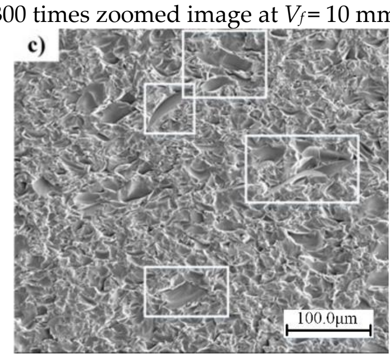

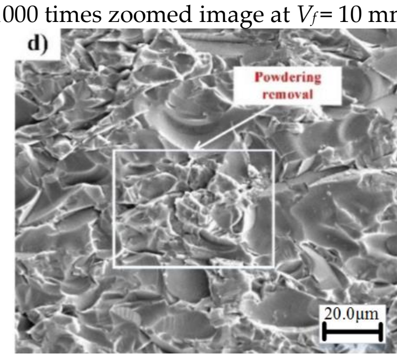

(**c**) 300 times zoomed image at V_f = 110 mm/min (**d**) 1000 times zoomed image at V_f = 110 mm/min

Figure 4. Machined surface morphologies of optical glass material at different feed rate.

The influence law of grinding depth on surface roughness is shown in Figure 5. It can be seen that as grinding depth increases, the surface roughness also tends to increase. A possible reason is that the value of grinding depth is strongly related to the magnitude of grinding force and penetration depth. Another reason is that the critical cutting depth of glass material is strongly affected by the grinding depth [26]. As grinding depth increases, it would be much easier for the transferring of material removal mode from ductile removal to brittle removal. Both two reasons mentioned above will lead to the influencing results shown in Figure 5.

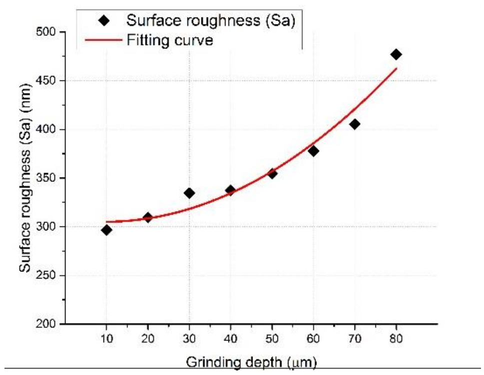

Figure 5. Influence of grinding depth on surface roughness.

Figure 6 shows the SEM images of machined surface morphologies of optical glass material zoomed by different times in different grinding depth. From Figure 6a,c, it can be seen that, as the grinding depth changed from 10 μm to 80 μm, the amount of brittle-fractured pits in large sizes increases, as shown in in Figure 6c, but not very obvious. And through the further observation on surface morphologies zoomed by 1000 times, as shown in Figure 6b,d, the morphologies of machined surface is found to be quite similar. They were both mainly removed by little ductile removal pits and quite a few brittle-fractured pits, supplemented removed by scraps in sub-micron level. No obvious lumps in micron level are found on the machined surfaces. Thus, while the feed rate maintains a relative higher level, the fracture lumps in micron level cannot take a large proportion whether the grinding depth is big or not.

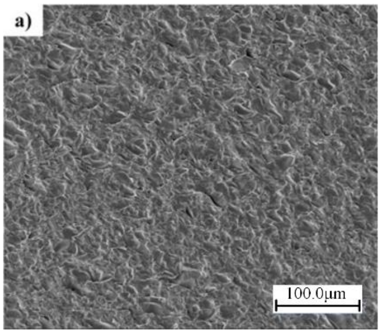

(**a**) 300 times zoomed image at a_p = 10 μm

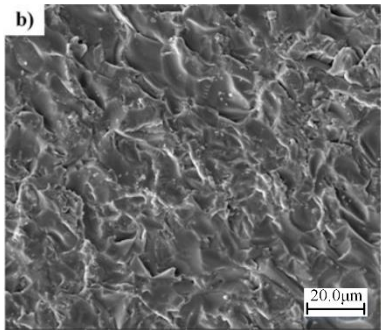

(**b**) 1000 times zoomed image at a_p = 10 μm

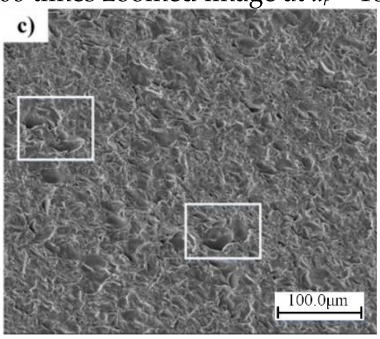

(**c**) 300 times zoomed image at a_p = 80 μm

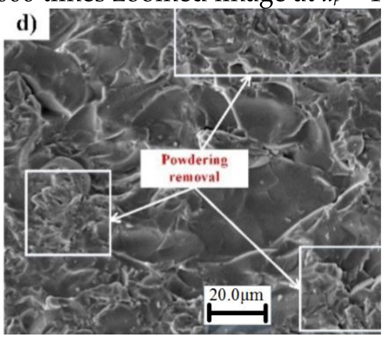

(**d**) 1000 times zoomed image at a_p = 80 μm

Figure 6. Machined surface morphologies of optical glass material at different grinding depth.

3.1.2. Effect of Ultrasonic Amplitude on Surface Morphologies and Surface Roughness

Ultrasonic vibration can provide separation effect between grinding tool and glass workpiece, and also can affect grinding force, critical cutting depth, and many other factors. Thus, it is necessary to investigate the influence of ultrasonic vibration on surface roughness and material removal mechanism.

The influence of ultrasonic vibration amplitude on surface roughness is shown in Figure 7. It is found that the surface roughness decreases as the ultrasonic vibration amplitude increases. A possible reason is that, the material removal process is much similar to that in conventional grinding while the ultrasonic vibration amplitude is in small value, the advantages of separation effect mentioned above cannot be reflected. Besides, the removal volume of a single abrasive grain would increase with a decrease in the separation effect. Another reason is that, the comprehensive and repeated impact and ironing pressing effects of abrasive grains on glass workpiece are weakened when ultrasonic amplitude is small, the motion strength of abrasive grains along axis direction is also weakened. The third reason it that, ultrasonic vibration can provide cracks shield effect, that is, the second indentation will not cause a median crack or this median crack will not propagate entirely if the distance between the first indentation and the second indentation is too small. If ultrasonic vibration amplitude is in small value, this effect will be restrained, the interference of median crack thus becomes weak, the lateral crack and brittle-fractured sizes will correspondingly become large, the surface roughness thus becomes large.

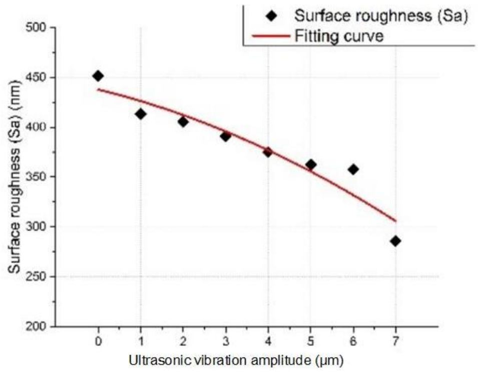

Figure 7. Influence of ultrasonic vibration amplitude on surface roughness.

Figure 8 showed the machined surfaces morphologies of BK7 optical glass material zoomed by different times and in different ultrasonic vibration status. Through the macro observation on Figure 8a,c, it is found the amount of ductile and brittle-fractured pits increases to a certain level when ultrasonic vibration was introduced into grinding process. 1000 times zoomed images are used in order to further observe the differences of morphologies and material removal modes. It can be seen from Figure 8b that, while the material was machined without the help of ultrasonic vibration, machined surface would consist of comprehensively distributed ductile, brittle-fractured pits, and their combinations. The powdering removal also can be obviously found to be in a large proportion, including fracture lumps in micron level and scraps in sub-micron level which covered the machined surface.

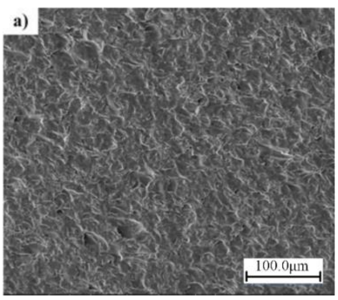

(**a**) 300 times zoomed image without ultrasonic vibration

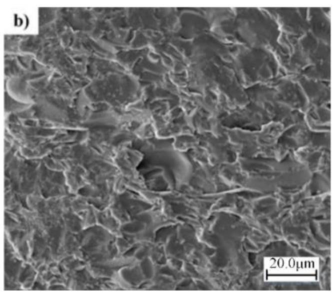

(**b**) 1000 times zoomed image without ultrasonic vibration

Figure 8. *Cont.*

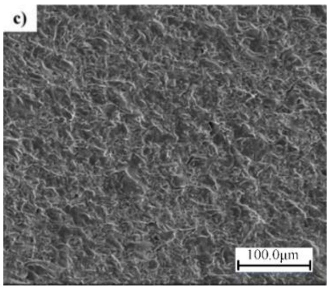

(**c**) 300 times zoomed image at $A = 7$ μm

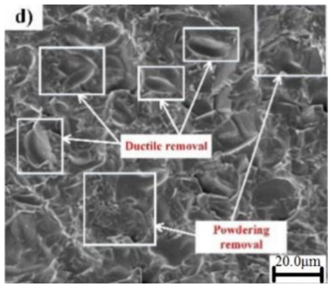

(**d**) 1000 times zoomed image at $A = 7$ μm

Figure 8. Machined surface morphologies of optical glass material at different ultrasonic vibration status.

After ultrasonic vibration was introduced into the grinding process, the material removal mechanism obviously changed. From Figure 8d, when ultrasonic vibration amplitude is 7 μm, the amounts of brittle-fractured pits in large sizes become much less, instead, ductile removal pits are induced. Meanwhile, the powdering removal in sub-micron level nearly disappear. The fracture lumps in micron level still have a certain proportion, but their amounts become much less. Instead of covering the machined surface in conventional grinding process, these powdering removal defects still connected to the machined surface.

Hence, a conclusion can be drawn that the introduction of ultrasonic vibration changes the proportion of three material removal modes (i.e., ductile removal, brittle removal and powdering removal). Besides, the proportion of ductile removal mode increases while the proportion of brittle removal mode decreases. The powdering removal in sub-micron level are strongly restrained by ultrasonic vibration, the proportion of fracture lumps in micron level decreases. Unlike conventional grinding, fracture lumps in micron level are still connected to the workpiece surface after machining, they did not separate the workpiece neither covered it.

3.2. Effect of Grinding and Ultrasonic Parameters on Surface Composition

The machined surface of ultrasonic vibration assisted grinding of BK7 optical glass consists of different proportions of ductile, brittle, and powdering areas. Understanding the increase in proportion of ductile removal, reduce the proportion of powder removal and brittle removal would help to improve the machined surface quality and clarify the direction of process optimization. Therefore, based on the above analysis, the effect of process parameters on the surface topography composition during ultrasonic vibration-assisted grinding of BK7 optical glass was summarized, as shown in the Figure 9.

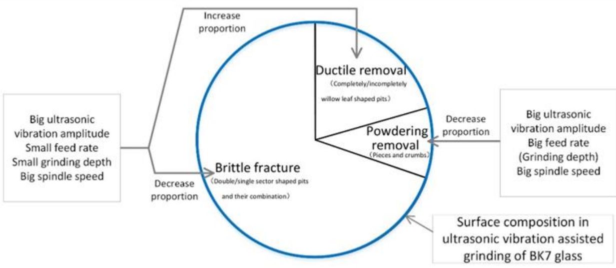

Figure 9. Effect of processing parameters on surface composition in ultrasonic vibration assisted grinding of optical glass BK7.

Figure 9 briefly summarizes the effect of ultrasonic vibration parameters and grinding parameters on the proportion of ductile removal, powdering removal, and brittle fracture. It is believed that brittle fracture always occupies the biggest proportion on the machined surfaces, while that of powdering removal is the smallest.

When the ultrasonic vibration amplitude and the spindle rotation speed are high the feed rate and the grinding depth are small, the ductile removal in the machined surface occupies a higher proportion. However, the changing of grinding wheel diameter did not show any obvious effect on the proportion of ductile removal and brittle fracture. However, the bigger the ultrasonic vibration amplitude is, the more obvious the repeated impact and ironing pressing effects are. Because of the high brittleness and low fracture toughness, excessive impact and force would lead to the rapid growth in sizes of surface and subsurface cracks. These disadvantages may cause the surface and subsurface qualities to decrease, thus, the limiting value of ultrasonic vibration amplitude in the effect to surface composition is 7 μm. The feed rate has the dominant effect to powdering removal, and the grinding depth has no obvious effect on the powdering removal. The lower feed rate would increase the proportion of powdering removal to a certain degree; changing of grinding depth has little effect on the proportion of powdering removal.

3.3. Analysis of the Changes in Surface Morphologies and Surface Roughness

Based on the above analysis, a better understanding on the mutual and comprehensive influence of grinding and ultrasonic vibration parameters on surface roughness was obtained, as shown in Figure 10.

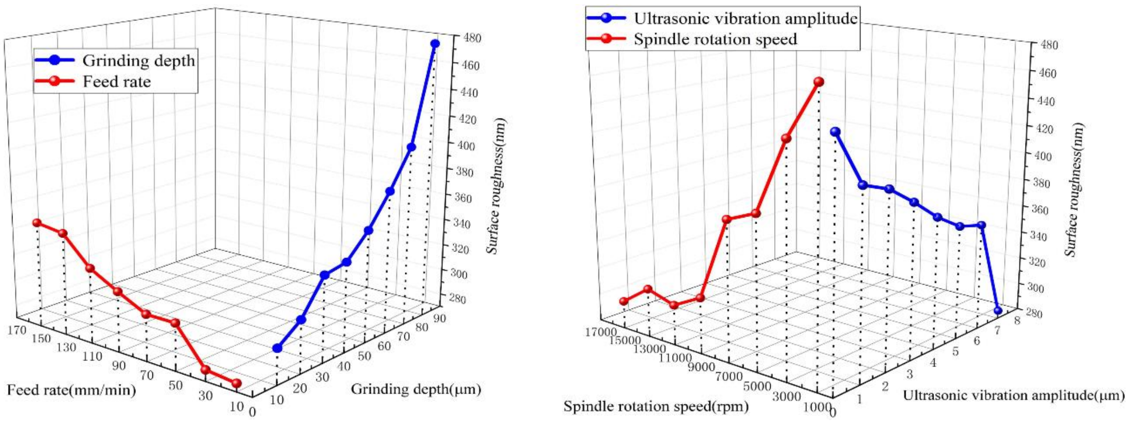

(**a**) Grinding depth and feed rate (**b**) Spindle rotation speed and ultrasonic amplitude

Figure 10. Influence of grinding and ultrasonic vibration parameters on the surface roughness in 3D space.

It can be seen from Figure 10a, in the grinding condition of these experiments, the rise in both grinding depth and feed rate could lead to an increase in the surface roughness. Among them, grinding depth has the dominant effect on surface roughness. It is because grinding depth mainly affect the proportion of brittle fracture and ductile removal, and these two material removal modes are the dominant effect to surface roughness, on the contrary, feed rate could affect the proportion of all the three removal modes, thus, the effect of feed rate on the brittle fracture and ductile removal would be weakened.

From Figure 10b, it can be seen that, the raise in both ultrasonic vibration amplitude and spindle rotation speed could lead to the sharp decrease in surface roughness. Besides, the influence degree to the surface roughness are much similar. However, the obvious influence of spindle rotation speed on surface roughness mainly was reflected in the initial stage, while that of ultrasonic vibration amplitude was reflected in both initial and later stages. The possible reason is that when spindle rotation speed increases initially, the amount of brittle-fractured pits and powdering removal reduces sharply, but the changes in removal volume of single abrasive grain tend to be smooth, thus the surface roughness would not continuously decrease sharply. On the other hand, the introduction of ultrasonic vibration leads to an obvious increase in the critical cutting depth, also the proportion of ductile removal, and with the increase in ultrasonic amplitude, this advantage becomes much more obvious, a sharp decrease in surface roughness finally comes to an end.

4. Conclusions

In this work, ultrasonic vibration-assisted grinding experiments of BK7 glass were carried out. According to the analysis of experimental results, the following conclusion can be obtained.

1. Machining parameters significantly influence the surface roughness (*Sa*). The surface roughness (*Sa*) and pits sizes increase with the increase in feed rate and grinding depth, and decrease with the increase in the spindle rotation speed and ultrasonic vibration amplitude.
2. Increase in spindle rotation speed and ultrasonic vibration amplitude, decrease in grinding depth and feed rate could increase the proportion of ductile removal and reduce the proportion of brittle removal. The introduction of ultrasonic vibration would largely inhibit the powder removal of submicron crumbs and reduce the proportion of powdered removal of micron-sized pieces. At the same time, the proportion of the ductile removal of willow leaf shaped removal could be increased, and the proportion of the brittle removal of sector shaped removal could be reduced.
3. Compared to feed rate, grinding depth has the dominant positive effect on the surface roughness, the reason is the difference in the effect degree of these two parameters to powdering removal proportion. The sharp decrease in proportion of brittle fracture and powdering removal is the reason of the initial obvious influence of spindle rotation speed on surface roughness. Surface roughness decreased obviously in both initial and later stages of increase in ultrasonic amplitude, the reason is the notable increase in proportion of ductile removal and the inhibition of powdering removal.

Author Contributions: Conceptualization, P.Y.Z.; Investigation, M.Z.; Software, X.L.L.; Validation, B.J.; Writing—original draft, P.Y.Z. All authors have read and agreed to the published version of the manuscript.

Funding: This research was funded by the National Natural Science Foundation of China] grant number [U1630104].

Conflicts of Interest: The authors declare no conflict of interest.

Nomenclature

Sa	Surface roughness (nm)
n	Spindle rotation speed (rpm)
V_f	Feed rate (mm/min)
a_p	Grinding depth (μm)
A	Ultrasonic amplitude (μm)

References

1. Xie, J.; Deng, Z.J.; Liao, J.Y.; Li, N.; Zhou, H.; Ban, W.X. Study on a 5-axis precision and mirror grinding of glass freeform surface without on-machine wheel-profile truing. *Int. J. Mach. Tools Manuf.* **2016**, *109*, 65–73. [CrossRef]
2. Cheng, J.; Wang, C.; Wen, X.L.; Gong, Y.D. Modeling and experimental study on micro-fracture behavior and restraining technology in micro-grinding of glass. *Int. J. Mach. Tools Manuf.* **2014**, *85*, 36–48. [CrossRef]
3. Belkhir, N.; Aliouane, T.; Bouzid, D. Correlation between contact surface and friction during the optical glass polishing. *Appl. Surf. Sci.* **2014**, *288*, 208–214. [CrossRef]
4. Shen, N.; Suratwala, T.; Steele, W.; Wong, L.; Feit, M.D.; Miller, P.E.; Dylla-Spears, R.; Desjardin, R. Nanoscratching of Optical Glass Surfaces Near the Elastic–Plastic Load Boundary to Mimic the Mechanics of Polishing Particles. *J. Am. Ceram. Soc.* **2016**, *99*, 1477–1484. [CrossRef]
5. Chen, J.; Fang, Q.; Li, P. Effect of grinding wheel spindle vibration on surface roughness and subsurface damage in brittle material grinding. *Int. J. Mach. Tools Manuf.* **2015**, *91*, 12–23. [CrossRef]

6. Xiao, H.; Wang, H.; Chen, Z.; Fu, G.; Wang, J. Effect of brittle scratches on transmission of optical glass and its induced light intensification during the chemical etching. *Opt. Eng.* **2017**, *56*, 105101. [CrossRef]
7. Liu, K.; Li, X.P.; Rahman, M. Characteristics of ultrasonic vibration-assisted ductile mode cutting of tungsten carbide. *Int. J. Adv. Manuf. Technol.* **2008**, *35*, 833–841. [CrossRef]
8. Fang, F.; Hao, N.; Hu, G. Rotary Ultrasonic Machining of Hard and Brittle Materials. *Nanotechnol. Precis. Eng.* **2014**, *12*, 227–234.
9. Mahaddalkar, P.M.; Miller, M.H. Force and thermal effects in vibration-assisted grinding. *Int. J. Adv. Manuf. Technol.* **2014**, *71*, 1117–1122. [CrossRef]
10. Zhang, J.H.; Zhao, Y.; Tian, F.Q.; Zhang, S.; Guo, L.S. Kinematics and experimental study on ultrasonic vibration-assisted micro end grinding of silica glass. *Int. J. Adv. Manuf. Technol.* **2015**, *78*, 1893–1904. [CrossRef]
11. Suárez, A.; Veiga, F.; De Lacalle, L.N.L.; Polvorosa, R.; Lutze, S.; Wretland, A. Effects of Ultrasonics-Assisted Face Milling on Surface Integrity and Fatigue Life of Ni-Alloy 718. *J. Mater. Eng. Perform.* **2016**, *25*, 5076–5086. [CrossRef]
12. Celaya, A.; De Lacalle, L.N.L.; Campa, F.J.; Lamikiz, A. Ultrasonic Assisted Turning of mild steels. *Int. J. Mater. Prod. Technol.* **2010**, *37*, 60. [CrossRef]
13. Feng, P.; Liang, G.; Zhang, J. Ultrasonic vibration-assisted scratch characteristics of silicon carbide-reinforced aluminum matrix composites. *Ceram. Int.* **2014**, *40*, 10817–10823. [CrossRef]
14. Tesfay, H.D.; Xu, Z.; Li, Z.C. Ultrasonic vibration assisted grinding of bio-ceramic materials: An experimental study on edge chippings with Hertzian indentation tests. *Int. J. Adv. Manuf. Technol.* **2016**, *86*, 3483–3494. [CrossRef]
15. Wang, J.; Guo, B.; Zhao, Q.; Zhang, C.Y.; Zhang, Q.L.; Zhai, W.J. Evolution of material removal modes of sapphire under varied scratching depths. *Ceram. Int.* **2017**, *43*, 10353–10360. [CrossRef]
16. Cao, J.G.; Wu, Y.B.; Guo, H.R.; Fujimoto, M.; Mitsuyoshi, N. Experimental investigation of material removal mechanism in ultrasonic assisted grinding of SiC ceramics using a single diamond tool. *Int. J. Mach. Tools Manuf.* **2013**, *7*, 93–96. [CrossRef]
17. Zhang, F.H.; Li, C.; Meng, B.B.; Zhao, H.; Liu, Z.D. Investigation of Surface Deformation Characteristic and Removal Mechanism for K9 Glass Based on Varied Cutting-depth Nano-scratch. *J. Mech. Eng.* **2016**, *52*, 65–71. [CrossRef]
18. Li, C.; Zhang, F.H.; Meng, B.B.; Liu, L.F.; Rao, X.S. Material removal mechanism and grinding force modelling of ultrasonic vibration assisted grinding for SiC ceramics. *Ceram. Int.* **2016**, *43*, 2981–2993. [CrossRef]
19. Zhang, F.H.; Li, C.; Zhao, H.; Leng, B.; Ren, L.L. Simulation and experiment of double grits interacting scratch for optical glass BK7. *J. Wuhan Univ. Technol. (Mater. Sci. Ed.)* **2018**, *33*, 15–22. [CrossRef]
20. Li, Z.P.; Zhao, H.; Zhang, F.H. Study on the Ductile Removal Behavior of K9 Glass with Nano-Scratch. *Adv. Mater. Res.* **2016**, *1136*, 282–288. [CrossRef]
21. Wang, W.; Yao, P.; Wang, J.; Huang, C.Z.; Zhu, H.T.; Liu, H.L.; Zou, B.; Liu, Y. Controlled material removal mode and depth of micro cracks in precision grinding of fused silica—A theoretical model and experimental verification. *Ceram. Int.* **2017**, *43*, 11596–11609. [CrossRef]
22. Dai, J.B.; Su, H.H.; Yu, T.F.; Hu, H.; Zhou, W.B.; Ding, W.F. Experimental investigation on the material removal mechanism in during grinding silicon carbide ceramics with single diamond grain. *Precis. Eng.* **2017**, *51*, 217–279. [CrossRef]
23. Gu, W.; Yao, Z.; Liang, X. Material removal of optical glass BK7 during single and double scratch tests. *Wear* **2011**, *270*, 241–246. [CrossRef]
24. Xiao, H.P.; Chen, Z.; Wang, H.R.; Wang, J.H.; Zhu, N. Effect of grinding parameters on surface roughness and subsurface damage and their evaluation in fused silica. *Opt. Express* **2018**, *26*, 4638–4655. [CrossRef]
25. Yu, T.; Li, H.; Wang, W. Experimental investigation on grinding characteristics of optical glass BK7: With special emphasis on the effects of machining parameters. *Int. J. Adv. Manuf. Technol.* **2016**, *82*, 1405–1419. [CrossRef]
26. Lv, D.X.; Huang, Y.H.; Tang, Y.J.; Wang, H.X. Relationship between subsurface damage and surface roughness of glass BK7 in rotary ultrasonic machining and conventional grinding processes. *Int. J. Adv. Manuf. Technol.* **2013**, *67*, 613–622. [CrossRef]
27. Pal, R.K.; Garg, H.; Sarepaka RG, V.; Karar, V. Experimental Investigation of Material Removal and Surface Roughness during Optical Glass Polishing. *Adv. Manuf. Process.* **2015**, *31*, 1613–1620. [CrossRef]

28. Lin, X.H.; Zhang, J.B.; Tang, H.H.; Du, X.Y.; Guo, Y.B. Analysis of surface errors and subsurface damage in flexible grinding of optical fused silica. *Int. J. Adv. Manuf. Technol.* **2017**, *88*, 643–649. [CrossRef]
29. Pereverzev, P.P.; Pimenov, D.Y.A. Grinding force model allowing for dulling of abrasive wheel cutting grains in plunge cylindrical grinding. *J. Frict. Wear* **2016**, *37*, 60–65. [CrossRef]
30. Jiang, C.; Wu, T.; Ye, H.; Cheng, J.; Hao, Y. Estimation of Energy and Time Savings in Optical Glass Manufacturing When Using Ultrasonic Vibration-Assisted Grinding. *Int. J. Precis. Eng. Manuf. Green Technol.* **2019**, *6*, 1–9. [CrossRef]
31. Zhao, P.Y.; Zhou, M.; Huang, S.N. Sub-surface crack formation in ultrasonic vibration-assisted grinding of BK7 optical glass. *Int. J. Adv. Manuf. Technol.* **2017**, *93*, 1685–1697. [CrossRef]
32. Rinck, P.M.; Sitzberger, S.; Zaeh, M.F. Actuator design for vibration assisted machining of high performance materials with ultrasonically modulated cutting speed. In Proceedings of the Fourth European Seminar on Precision Optics Manufacturing, International Society for Optics and Photonics, Teisnach, Germany, 4–5 April 2017; Volume 103260C. [CrossRef]
33. Liu, L.P.; Zhao, W.; Ma, Y. Study on Imitating Grinding of Two-Dimensional Ultrasonic Vibration Turning System. In *International Conference on Computer and Computing Technologies in Agriculture, Nanchang, China, 22–25 October 2010*; Springer: Berlin/Heidelberg, Germany, 2010; pp. 333–344. [CrossRef]
34. Zhou, M.; Zhao, P.Y. Prediction of critical cutting depth for ductile-brittle transition in ultrasonic vibration assisted grinding of optical glasses. *Int. J. Adv. Manuf. Technol.* **2016**, *86*, 1775–1784. [CrossRef]